Quantum Spin Hall Effect in Inverted Type-II Semiconductors

Chaoxing Liu,[1,2] Taylor L. Hughes,[2] Xiao-Liang Qi,[2] Kang Wang,[3] and Shou-Cheng Zhang[2]
[1]*Center for Advanced Study, Tsinghua University, Beijing, 100084, China*
[2]*Department of Physics, McCullough Building, Stanford University, Stanford, California 94305-4045, USA*
[3]*Department of Electrical Engineering, UCLA, Los Angeles, California 90095-1594, USA*
(Received 24 January 2008; published 11 June 2008)

The quantum spin Hall (QSH) state is a topologically nontrivial state of quantum matter which preserves time-reversal symmetry; it has an energy gap in the bulk, but topologically robust gapless states at the edge. Recently, this novel effect has been predicted and observed in HgTe quantum wells and in this Letter we predict a similar effect arising in Type-II semiconductor quantum wells made from InAs/GaSb/AlSb. The quantum well exhibits an ''inverted'' phase similar to HgTe/CdTe quantum wells, which is a QSH state when the Fermi level lies inside the gap. Due to the asymmetric structure of this quantum well, the effects of inversion symmetry breaking are essential. Remarkably, the topological quantum phase transition between the conventional insulating state and the quantum spin Hall state can be continuously tuned by the gate voltage, enabling quantitative investigation of this novel phase transition.

DOI: 10.1103/PhysRevLett.100.236601 PACS numbers: 72.20.−i, 72.25.Dc, 73.63.Hs

Recently, a striking prediction of a quantum spin Hall (QSH) insulator phase in HgTe/CdTe quantum wells (QW) [1] was confirmed in transport experiments [2]. The QSH phase [3,4] is a topologically nontrivial state of matter reminiscent of the integer quantum Hall effect, but where time-reversal symmetry is preserved instead of being broken by the large magnetic field. The state is characterized by a bulk charge-excitation gap and topologically protected helical edge states, where states of opposite spin counterpropagate on each edge [3,5,6]. Unfortunately, high-quality HgTe/CdTe QW are very special, and only a few academic research groups have the precise material control needed to carry out such delicate experiments. We are therefore lead to search for other, more conventional, materials that exhibit the QSH effect.

We introduce a new material with the QSH phase: InAs/GaSb/AlSb Type-II semiconductor QW in the inverted regime [7–12]. We show that this quantum well has a subband inversion transition as a function of layer thickness, similar to the HgTe/CdTe system, and can be characterized by an effective four-band model near the transition. This model is similar to the model for HgTe/CdTe [1], but contains terms describing the strong bulk inversion asymmetry (BIA) and structural inversion asymmetry (SIA). In fact, due to the unique band alignment of InAs/GaSb/AlSb, the electron subband and the hole subband are localized in *different* quantum well layers. Treated within the self-consistent formalism [13–15], the intrinsic asymmetry and the band alignment leads to novel effects which we discuss below.

After the demonstration of the QSH state, the key fundamental question concerns the nature of the topological quantum phase transition between the conventional insulating state and the QSH state. Unfortunately, in HgTe quantum wells, this phase transition can only be tuned by the thickness of the quantum well, which is a discrete variable. In this work, we show that the asymmetric InAs/GaSb/AlSb quantum well, with strong built-in electric field, can be electrically tuned through the phase transition using front and back gates. Therefore, this system offers the unique possibility to quantitatively investigate the topological quantum phase transition by continuously tuning the gate voltage. Additionally, this system also allows one to construct a quantum spin Hall field effect transistor (FET), where the gate voltage can switch between the ''OFF'' state of a conventional insulating state, and a nearly dissipationless ''ON'' state with the conducting edge channels of the QSH state.

The QW structures in which we are interested are asymmetric with AlSb/InAs/GaSb/AlSb layers grown as shown in Fig. 1. This is an unusual QW system due to the alignment of the conduction and valence band edges of InAs and GaSb. The valence band edge of GaSb is 0.15 eV *higher* than the conduction band edge of the InAs layer. The AlSb layers serve as confining outer barriers. The ''conduction'' subbands are localized in the InAs layer while the ''valence'' subbands are localized in the GaSb layer as illustrated in Fig. 1(a). Here we focus on the regime where the lowest electron and hole subbands E_1, H_1, which are derived from the s-like conduction and p-like heavy-hole bands, respectively, are nearly degenerate, and all other subbands are well separated in energy. When the quantum well thickness is increased the E_1 (H_1) band edge decreases (increases). At a critical thickness a level crossing occurs between E_1 and H_1, after which the band edge of E_1 sinks below that of H_1, putting the system into the inverted regime of Type-II QW. Since the H_1 band disperses downwards and the E_1 band disperses upwards, the inversion of the band sequence leads to a crossing of the two bands; see Fig. 1(b). Historically, the inverted regime of InAs/GaSb/AlSb QW was described as a semimetal without a gap [7]. However, Ref. [8] first pointed out that due to the mixing between E_1 and H_1, a small gap [E_g in Fig. 1(b)] is generally opened, leading to bulk insulating

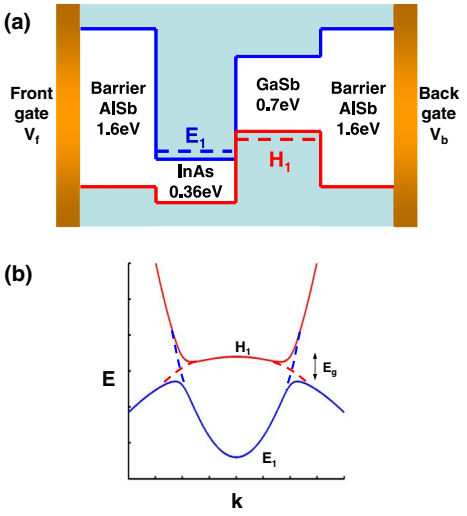

FIG. 1 (color online). (a) Band gap and band offset diagram for asymmetric AlSb/InAs/GaSb quantum wells. The left AlSb barrier layer is connected to a front gate while the right barrier is connected to a back gate. The E_1 subband is localized in the InAs layer and H_1 is localized in the GaSb layer. Outer AlSb barriers provide an overall confining potential for electron and hole states. (b) Schematic band structure diagram. The dashed line shows the crossing of E_1 and H_1 in the inverted regime. Hybridization between E_1 and H_1, opens the gap E_g.

behavior. This hybridization gap was later demonstrated in experiments [9,10]. Therefore, just like in the HgTe/CdTe QW, the inverted regime of InAs/GaSb QW should be a topologically nontrivial QSH phase protected by the bulk gap.

This simple conclusion is complicated by the unique features of type-II QW: the electron subband and hole subband are separated in two different layers. There are several separate consequences of this fact. First, the hybridization between E_1 and H_1 is reduced, but this is just a quantitative correction. Second, since there is no inversion symmetry in the quantum well growth direction, SIA terms may be large enough to compete with the reduced hybridization. In addition, BIA may also play a role. Therefore, both SIA and BIA must be included properly to make a correct prediction, while in HgTe/CdTe QW these two types of terms were ignored because BIA terms are small when compared with the gap, and the QW were symmetric which minimizes SIA. Finally, since the electron and hole subbands lie in two different layers, there is an automatic charge transfer between the layers which yields a coexistence of p-type and n-type carriers. Consequently, a self-consistent treatment of Coulomb energy is necessary to account for this effect. We will discuss all of these issues and conclude that the QSH phase exists in an experimentally viable parameter range.

These bulk systems have zinc-blende lattice structure and direct gaps near the Γ point and are thus well described by the 8-band Kane model [16]. We will construct an effective 4-band model using the same procedure as the Bernevig-Hughes-Zhang (BHZ) model [1], albeit a more complex one due to the SIA and BIA terms. The Hamiltonian naturally separates into three parts:

$$\mathcal{H} = H_0 + H_{\mathrm{BIA}} + H_{\mathrm{SIA}}. \tag{1}$$

In the basis $\{|E_1+\rangle, |H_1+\rangle, |E_1-\rangle, |H_1-\rangle\}$, and keeping terms only up to quadratic powers of $\mathbf{k}$, we have

$$H_0 = \epsilon(k)\mathbf{I}_{4\times 4} + \begin{pmatrix} \mathcal{M}(k) & Ak_+ & 0 & 0 \\ Ak_- & -\mathcal{M}(k) & 0 & 0 \\ 0 & 0 & \mathcal{M}(k) & -Ak_- \\ 0 & 0 & -Ak_+ & -\mathcal{M}(k) \end{pmatrix}, \tag{2}$$

where $\mathbf{I}_{4\times 4}$ is the 4×4 identity matrix, $\mathcal{M}(k) = M_0 + M_2k^2$ and $\epsilon(k) = C_0 + C_2k^2$. This is simply the Hamiltonian used by BHZ. Two different atoms in each unit cell breaks bulk inversion symmetry and leads to additional terms [17]. When projected onto the lowest subbands the BIA terms are

$$H_{\mathrm{BIA}} = \begin{pmatrix} 0 & 0 & \Delta_e k_+ & -\Delta_0 \\ 0 & 0 & \Delta_0 & \Delta_h k_- \\ \Delta_e k_- & \Delta_0 & 0 & 0 \\ -\Delta_0 & \Delta_h k_+ & 0 & 0 \end{pmatrix}. \tag{3}$$

Finally, the SIA term reads

$$H_{\mathrm{SIA}} = \begin{pmatrix} 0 & 0 & i\xi_e k_- & 0 \\ 0 & 0 & 0 & 0 \\ -i\xi_e^* k_+ & 0 & 0 & 0 \\ 0 & 0 & 0 & 0 \end{pmatrix}. \tag{4}$$

Here we recognize the SIA term as the electron k-linear Rashba term; the heavy-hole k-cubic Rashba term is neglected. The parameters Δ_h, Δ_e, Δ_0, ξ_e depend on the quantum well geometry.

Now we address the QSH phase transition. Without H_{BIA} and H_{SIA} the Hamiltonian is block diagonal and each block is exactly a massive Dirac Hamiltonian in $(2+1)d$. This is the BHZ model and from their argument we know that there is a topological phase transition signaled by the gap-closing condition $M_0 = 0$, and the system is in QSH phase when $M_0/M_2 < 0$. When H_{BIA} and H_{SIA} terms are included, the two blocks of H_0 are coupled together and the analysis does not directly apply. However, the QSH phase is a topological phase of matter protected by the band gap [3,5,6]. If we start from the Hamiltonian H_0 in the QSH phase and turn on H_{BIA} and H_{SIA} adiabatically, the system will remain in the QSH phase as long as the energy gap between E_1 and H_1 remains finite. With realistic parameters for InAs/GaSb/AlSb QW obtained from the 8-band Kane model, the adiabatic connection between H_0 and the full Hamiltonian $\mathcal{H}$ was verified for the proper parameter regime, which supports the existence of a QSH phase in this system. Though the BIA and SIA terms do not destroy the QSH phase, they do modify the quantum phase transition between the QSH phase and normal insulator (NI). The transition (gap-closing) will generically occur at

finite-$\mathbf{k}$ rather than at the Γ point, and a nodal region between QSH and NI phases can possibly appear in the phase diagram [18–21].

A more direct way of identifying the QSH phase is to study the edge state spectrum. There are always an odd number of Kramers's pairs of edge states on the boundary of a QSH insulator, and an even number pairs (possibly zero) for the boundary of a NI. The edge state energy spectrum of the effective model (1) can be obtained by solving this model with a simple tight-binding regularization in a cylindrical geometry. The spectrum is shown in Fig. 2. We find one Kramers's pair of edge states with opposite spin per edge for the QSH side, and no edge states for the NI side. This confirms the existence of QSH phase in this model.

To study InAs/GaSb/AlSb QW more systematically and quantitatively, we confirm the above analysis by numerically solving the full 8-band Kane model. In the inverted regime, there exists an intrinsic charge transfer between the InAs layer and GaSb layer. Therefore, we need to take into account the built-in electric field. The energy dispersions for different well thicknesses are shown in Figs. 3(a)–3(c), where we fix the GaSb layer thickness $d_1 = 10$ nm and vary the thickness of InAs layer d_2. The system is gapped for a generic value of d_2. However, at a critical thickness $d_{2c} = 9$ nm [Fig. 3(b)] a crossing at finite $\mathbf{k}$ occurs between the subbands E_1 and H_1, which marks the phase transition between the QSH and NI phases. From the above adiabatic continuity argument, we know that QW are in a NI state for $d_2 < d_{2c}$ [Fig. 3(a)] and QSH state for $d_2 > d_{2c}$ [Fig. 3(c)]. As the band inversion is only determined by the relative positions of E_1 and H_1, the QW with other values of d_1 behave essentially the same. As the QSH and NI phases are always separated by a gap closing, we can determine the d_1-d_2 phase diagram via the energy gap. As shown in Fig. 3(d), two gapped regimes (in red) are separated by a critical line (brightly colored) in the d_1-d_2 plane. The quantum well configurations shown in Figs. 3(a)–3(c) are indicated by points A, B and C, respectively. Because of adiabatic continuity, an entire connected gapped region in the phase diagram is in the NI (QSH) phase once one point in it is confirmed to be in this phase. Since Fig. 3(a) corresponds to the NI phase and (c) the QSH phase, we identify the right side of the diagram as QSH the left side as NI.

A major advantage of InAs/GaSb/AlSb QW is that due to the large built-in electric field, the QSH-NI phase transition can be easily tuned by external gate voltages. Tuning a gate voltage adjusts the band structure and Fermi level simultaneously. Since the QSH effect can only occur when the Fermi level lies in the gap, we need two gates to independently tune the relative position between the E_1 and H_1 band edges and the Fermi level. Such a dual-gate geometry has already been realized experimentally in InAs/GaSb/AlSb QW [11]. We performed a self-consistent Poisson-Schrodinger calculation [13–15] for such a dual-gate geometry shown in Fig. 1(a). To simplify the calculation, we made the thickness of the AlSb barrier layers much smaller than realistic experiments. This has a negligible effect for the QW except for a rescaling of V_f and V_b. We also neglect the weak effects of subband anisotropy and intrinsic donor defects at the InAs/GaSb interface. None of these simplifications should affect our results qualitatively.

For fixed $d_1 = d_2 = 10$ nm we explored the V_f-V_b phase diagram as shown in Fig. 4. There are six distinct regions in the figure. The dotted black line shows the phase boundary between the inverted and noninverted regimes. In parameter regions I, II, and III the system has an inverted band structure, but only region II is in the QSH phase with a Fermi level inside the bulk gap. Region I (III) is described by roughly the same spectrum as the QSH phase, but with

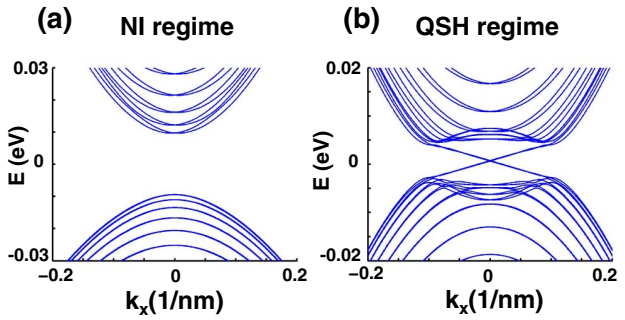

FIG. 2 (color online). Energy spectrum of Eq. (1) on a cylinder with open boundary conditions in the y-direction and periodic boundary conditions in the x-direction. (a) The dispersion for a quantum well with GaSb layer thickness $d_1 = 10$ nm, InAs layer thickness $d_2 = 8.1$ nm, which is a NI with no edge states. (b) The dispersion for a $d_1 = d_2 = 10$ nm quantum well which is a QSH insulator with one pair of edge states. A tight-binding regularization with lattice constant $a = 20$ Å was used.

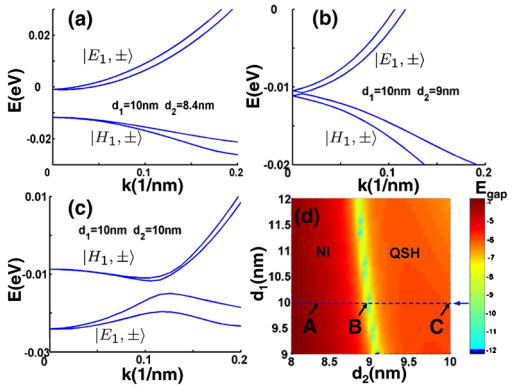

FIG. 3 (color online). (a)–(c) The energy dispersions calculated from the 8-band Kane model for three well configurations, where d_1 and d_2 are the thickness of GaSb layer and InAs layer, respectively. (d) The energy gap variation in d_1-d_2 plane, where brighter colors represent a smaller gap. A, B and C on the dashed blue line indicate, respectively, the place where (a),(b), and (c) are plotted. NI and QSH denote the phases in the corresponding region of parameter space.

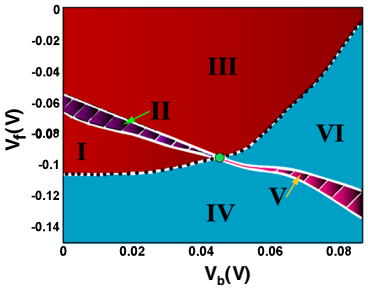

FIG. 4 (color online). Phase diagram for different front (V_f) and back (V_b) gate voltages. Regions I, II, III are in the inverted regime. The striped region II is the QSH phase with Fermi-level in the bulk gap, and I (III) is the $p(n)$-doped inverted system. Regions IV, V, VI are in the normal regime. The striped region V is the NI phase with Fermi level in the bulk gap, and IV (VI) is the $p(n)$-doped normal semiconductor. The black dotted line is the pase boundary between inverted and non-inverted band structures and the green circle shows the quantum critical point between the NI and QSH phases. The well configuration has $d_1 = d_2 = 10$ nm, and AlSb barrier thickness is 30 nm on each side. V_f and V_b are defined with respect to the Fermi levels of the QW.

finite $p(n)$-doping. Similarly region V is the NI phase and IV, VI are the corresponding p-doped and n-doped normal semiconductors. Thus, by tuning V_f and V_b to the correct range, one can easily control the phase transition between QSH(II) and NI(V). We highlight the direct quantum critical point between the QSH(II) and NI(V) phases in Fig. 4.

Compared to a similar proposal of a gate-induced phase transition in asymmetric HgTe/CdTe QW [22], InAs/GaSb/AlSb QW are much more sensitive to the gate voltage, which makes it much easier to realize such a transition experimentally. This is due to the fact that the electron and hole wavefunctions are centered in separate layers, so that the effect of the gate voltage on them is highly asymmetric. This simple mechanism allows us to investigate the quantum phase transition from the NI to the QSH state *in situ*, through the continuous variation of the gate voltage, rather than the discrete variation of the quantum well thickness. It is also useful for developing a QSH FET. The FET is in an "OFF" state when the Fermi level lies inside the normal insulating gap. Then, by adjusting the gate voltages the FET can be flipped to the "ON" state by passing through the transition to the QSH phase, where the current is carried only by the dissipationless edge states. This simple device can be operated with reasonable voltages as seen in Fig. 4 but would be more promising if one could enlarge the bulk insulating gap to support room temperature operation.

In conclusion, we propose that the QSH state can be realized in InAs/GaSb QW. We presented both simple arguments based on an effective model and realistic self-consistent calculations. We showed that this system has the distinct advantage over HgTe QW, in that the quantum phase transition can be continuously tuned by the gate voltage. This principle could be used to construct a QSH FET device with minimal dissipation.

We would like to thank T. P. Devereaux and B. F. Zhu for useful discussions. This work is supported by the NSF under Grant No. DMR-0342832, the U.S. Department of Energy, Office of Basic Energy Sciences under Contract DE-AC03-76SF00515, and by the Focus Center Research Program (FCRP) Center on Functional Engineered Nanoarchitectonics (FENA). C. X. L. acknowledges support of China Scholarship Council, NSF of China (Grants No. 10774086 and No. 10574076), Program of Basic Research Development of China (Grant No. 2006CB921500), and computing support from SHARCNET.

[1] B. A. Bernevig, T. L. Hughes, and S. C. Zhang, Science **314**, 1757 (2006).
[2] M. Konig, S. Wiedmann, C. Brune, A. Roth, H. Buhmann, L. W. Molenkamp, X.-L. Qi, and S.-C. Zhang, Science **318**, 766 (2007).
[3] C. L. Kane and E. J. Mele, Phys. Rev. Lett. **95**, 226801 (2005).
[4] B. A. Bernevig and S. C. Zhang, Phys. Rev. Lett. **96**, 106802 (2006).
[5] C. J. Wu, B. A. Bernevig, and S. C. Zhang, Phys. Rev. Lett. **96**, 106401 (2006).
[6] C. Xu and J. Moore, Phys. Rev. B **73**, 045322 (2006).
[7] L. L. Chang and L. Esaki, Surf. Sci. **98**, 70 (1980).
[8] M. Altarelli, Phys. Rev. B **28**, 842 (1983).
[9] M. J. Yang, C. H. Yang, B. R. Bennett, and B. V. Shanabrook, Phys. Rev. Lett. **78**, 4613 (1997).
[10] M. Lakrimi, S. Khym, R. J. Nicholas, D. M. Symons, F. M. Peeters, N. J. Mason, and P. J. Walker, Phys. Rev. Lett. **79**, 3034 (1997).
[11] L. J. Cooper, N. K. Patel, V. Drouot, E. H. Linfield, D. A. Ritchie, and M. Pepper, Phys. Rev. B **57**, 11 915 (1998).
[12] E. Halvorsen, Y. Galperin, and K. A. Chao, Phys. Rev. B **61**, 16 743 (2000).
[13] I. Lapushkin, A. Zakharova, S. T. Yen, and K. A. Chao, J. Phys. Condens. Matter **16**, 4677 (2004).
[14] I. Semenikhin, A. Zakharova, K. Nilsson, and K. A. Chao, Phys. Rev. B **76**, 035335 (2007).
[15] Y. Naveh and B. Laikhtman, Phys. Rev. Lett. **77**, 900 (1996).
[16] E. O. Kane, J. Phys. Chem. Solids **1**, 249 (1957).
[17] R. Winkler, *Spin-Orbit Coupling Effects in Two-Dimensional Electron and Hole Systems*, Springer Tracts in Modern Physics (Springer, New York, 2003).
[18] S. Murakami, S. Iso, Y. Avishai, M. Onoda, and N. Nagaosa, Phys. Rev. B **76**, 205304 (2007).
[19] X. Dai, T. L. Hughes, X.-L. Qi, Z. Fang, and S.-C. Zhang, arXiv:0705.1516 [Phys. Rev. B. (to be published)].
[20] M. Koenig, H. Buhmann, L. W. Molenkamp, T. L. Hughes, C.-X. Liu, X.-L. Qi, and S.-C. Zhang, arXiv:0801.0901.
[21] T. L. Hughes, C.-X. Liu, X.-L. Qi, and S.-C. Zhang (to be published).
[22] W. Yang, K. Chang, and S. C. Zhang, arXiv:0711.1900.